Journal of Chromatography A, 1217 (2010) 264–275

Contents lists available at ScienceDirect

Journal of Chromatography A

journal homepage: www.elsevier.com/locate/chroma

Features of the adsorption of Naproxen on the chiral stationary phase (*S*,*S*)-Whelk-O1 under reversed-phase conditions

Leonid Asnin[a,b,c], Fabrice Gritti[b,c], Krzysztof Kaczmarski[d], Georges Guiochon[b,c,*]

[a] *Institute of Technical Chemistry, the Ural Branch of the Russian Academy of Sciences, Perm 614990, Russia*
[b] *Department of Chemistry, University of Tennessee, 552 Buehler Hall, Knoxville, TN 37996-1600, USA*
[c] *Division of Chemical Sciences, Oak Ridge National Laboratory, Oak Ridge, TN 37831-6120, USA*
[d] *Faculty of Chemistry, Rzeszów University of Technology, 35-959 Rzeszów, Poland*

ARTICLE INFO

Article history:
Received 6 August 2009
Received in revised form 9 November 2009
Accepted 13 November 2009
Available online 27 November 2009

Keywords:
Adsorption isotherms
Naproxen
Pirkle phase
Whelk-O1

ABSTRACT

Using elution chromatography, we studied the adsorption mechanism of the Naproxen enantiomers on the chiral stationary phase (*S*,*S*)-Whelk-O1, from buffered methanol–water solutions. We propose an adsorption mechanism that assumes monolayer adsorption of the more retained enantiomer and the associative adsorption of the less retained one. The effects of the mobile phase composition on the adsorption of Naproxen are discussed. The combination of an elevated column temperature and of the use of an acidic mobile phase led to the degradation of the column and caused a major loss of its separation ability. The use of a moderately acidic mobile phase at temperature slightly above ambient did not produce rapid severe damages but, nevertheless, hampered the experiments and caused a slow gradual deterioration of the column.

1. Introduction

The resolution of the Naproxen enantiomers on a Whelk-O1 chiral stationary phase (CSP) (see Fig. 1) has become a classical example of direct chromatographic enantio-separation [1,2]. This CSP was the first Pirkle-type phase to be commercialized. It has been distributed for more than 20 years. Therefore, it is surprising that there is still little information on the macroscopic, let alone the microscopic retention mechanisms of the adsorption and separation of the Naproxen enantiomers on this adsorbent. Until now, the efforts of most analysts were focused on uncovering the nature of the enantio-recognition process taking place during the chromatographic analyses made with the chiral selector [3–9] and on studying the influence of the mobile phase composition on the retention and chiral resolution [10–13]. Although helpful for analytical purposes, this information contributes little to our understanding of the mechanism of adsorption beyond the linear part of the adsorption isotherm. Yet, knowledge of this mechanism would be of great importance for the development of preparative separations.

Most applications of Whelk-O1 include the enantio-separations of Naproxen and of a few other 2-arylpropionic acids. They were developed for normal-phase chromatography [1,14–18]. However, the reversed-phase mode of chromatography is more desirable for preparative separations of ionizable compounds because these have a higher solubility in aqueous solutions of organic solvents. Several examples of the use of this CSP with water-containing mobile phases are reported [17,19,20]. The retention of several chiral analytes in reversed-phase liquid chromatography (RPLC) and in the so-called polar organic mode were studied by the linear chromatography method [10,21,22]. In this report, we extend these investigations of the RPLC of Naproxen on Whelk-O1 by using the more informative nonlinear chromatography method that consists in measuring adsorption isotherms and analyzing the shape of overloaded bands [23].

2. Theory

2.1. The concepts of excess adsorption and of adsorption in finite-thickness layers

Adsorption in liquid/solid systems changes the concentrations of the solution components in the thin layer of liquid phase adjacent to the solid surface (if the solid is impermeable) that is affected by the adsorption force field. This change can be either positive (with respect to the bulk equilibrium concentration) when the preferentially adsorbed solutes concentrate near the solid surface or negative when the solution components are displaced from the surface region into the bulk phase. Since there is no experimental method to measure the distribution of a solute in the direction

* Corresponding author. Tel.: +1 865 974 0733; fax: +1 865 974 2667.
E-mail address: guiochon@utk.edu (G. Guiochon).

0021-9673/$ – see front matter © 2009 Elsevier B.V. All rights reserved.
doi:10.1016/j.chroma.2009.11.039

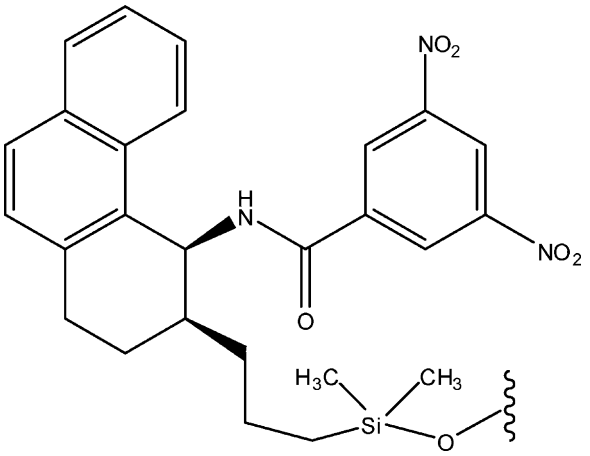

Fig. 1. Structure of the (*S,S*)-Whelk-O1 chiral selector.

perpendicular to the adsorbent surface nor to determine the thickness of the adsorbed layer, the determination of the composition of this adsorbed layer requires the selection of a model of the adsorbed phase. In contrast, it is easy to measure the differences of the concentrations before and after the equilibrium is established. This observation suggests the concept of excess adsorption which originates in the work of Gibbs [24].

In this approach, the adsorbed amount is considered to be the excess of solute contained in the real adsorption system compared with that in a hypothetical system in which the solute concentrations are uniform throughout the whole volume of the bulk mobile phase and equal to the equilibrium concentrations in the bulk phase of the real system. Defined in this way, this quantity can be experimentally measured, which requires no prior knowledge of the size, structure, and properties of the actual adsorbed phase. The operational definition of the excess adsorption for binary mixtures that is adopted in chromatography [25] is based on the condition of constancy of the volume of the liquid phase in the system, V_0:

$$\Gamma_i = \frac{(c_{0,i} - c_{e,i})V_0}{V_a} \tag{1}$$

where $c_{0,i}$ and $c_{e,i}$ are the concentrations of the component i before and after the equilibrium is established and V_a is the stationary phase volume. The isochoric restriction implies two assumptions:

(1) The molar volumes of the solution components are the same in both phases.
(2) No volume change takes place due to bulk mixing, i.e., the partial molar volumes of the solution components are equal to their molar volumes and do not depend on their concentrations.

The first assumption demands that the adsorbate molecules have the same volume both in the bulk solution and near the solid surface, where they are under the influence of the surface forces. This is a reasonable approximation for mesoporous adsorbents like Whelk-O1 and it has little influence on the accuracy of the calculations made with Eq. (1). The second assumption mandates the validity of the additivity rule when applied to the volume of the liquid phase. To a degree, it is a simplification because, in non-ideal solutions, the volumes corresponding to different concentrations (e.g., c_0 and c_e) can be different.

In adsorption studies, another definition of adsorption that considers the total amount of solute in a layer of finite thickness frequently appears to be convenient. This definition, which was developed by Guggenheim [26], supposes the existence of a hypothetical plane parallel to the adsorbent surface, at a distance τ from it. Above this plane, the component concentrations are supposed to be equal to the equilibrium concentrations. The total adsorbed amount of component i in the volume between this plane and the adsorbent surface per unit of adsorbent volume is

$$q_i = \frac{gS}{V_a} c_{e,i}\tau + \Gamma_i(c_{e,i}) \tag{2}$$

where g is the mass of adsorbent and S its specific surface area. Since there are no experimental methods to determine the analyte distribution in the direction normal to the surface, the assignment of τ relies on a conceptual model of the structure of the adsorbed phase and is frequently arbitrary.

2.2. Total adsorption isotherm models

In studies of the adsorption of mixtures of two infinitely miscible liquids, the equilibrium concentrations continuously varies through the whole range of solution composition, from zero to the concentration of a pure solute. In this case, there is always a region of high concentrations in which the product $c_{e,i}\tau$ is measurable compared to the excess adsorption and therefore cannot be neglected. On the contrary, the solute concentration in solutions of solids is restricted by the solubility of the solid, which is generally low enough to allow the assumption that the excess adsorption is equal to the total adsorbed amount. This allows the application of the stoichiometric method to the analysis of adsorption data. In the framework of this approach, adsorption equilibrium is described in terms of equilibrium quasichemical reactions. So, the simple addition reaction between solute B and adsorbent M

$$\mathrm{B} + \mathrm{M} \rightleftharpoons \mathrm{B\text{–}M} \tag{3}$$

results in the well known Langmuir isotherm

$$q = \frac{q^\star b c_e}{1 + b c_e} \tag{4}$$

where $q^\star$ is the concentration of adsorption sites and b is the equilibrium constant for Eq. (3) or adsorption coefficient. Any equilibrium process in either the liquid phase or on the adsorbent surface can be represented by a quasireaction scheme like Eq. (3) and included in the adsorption isotherm. It must be noted that the Langmuir model assumes that all the adsorption sites have the same affinity with respect to an adsorbate. In fact, solids are heterogeneous due to imperfections of the real surface and adsorption sites are characterized by a certain affinity distribution, with b being the average weighted coefficient for this distribution. If there exists a few types of adsorption sites on the surface, each group is distributed over a finite range of b-space, having their respective average b values.

In chiral chromatography, an adsorption model is often considered, in which two types of adsorption sites coexist on the stationary phase, enantioselective and nonselective sites. It is assumed that these sites can interact independently with a chiral analyte [27–29]. The enantioselective sites exhibit different affinity towards the two optical antipodes whereas the nonselective sites interact with both antipodes identically. The adsorption isotherm for this model (so-called the bi-Langmuir isotherm) is merely the sum of two Langmuir terms, one for each types of adsorption sites:

$$q = \frac{q^\star_{ns} b_{ns} c_e}{1 + b_{ns} c_e} + \frac{q^\star_s b_s c_e}{1 + b_s c_e} \tag{5}$$

The indices *ns* and *s* correspond to the nonselective and the selective adsorption sites, respectively. It is obvious that for the enantiomers (R) and (S), the following conditions are true: $b_{ns,R} = b_{ns,S} = b_{ns}$ and $b_{s,S} \neq b_{s,R}$. The equilibrium adsorption constant at infinite dilution (Henry coefficient, K_H) for this isotherm is given by the expression [27]:

$$K_H = q^\star_{ns} b_{ns} + q^\star_s b_s \tag{6}$$

3. Experimental

3.1. Apparatus

All the experiments made in this work were carried out using a HP 1090 Series II liquid chromatograph (Hewlett Packard, now Agilent Technologies, Palo Alto, CA), equipped with a multisolvent delivery system, an automatic injector, a column thermostat, a DAD detector, and a HP Chemstation data acquisition system. Chromatograms of Naproxen enantiomers were recorded using the standard DAD detector, otherwise a HP 1037A refractive index (RF) detector connected to the data acquisition system through an Agilent 35900E Interface was used. The extra-column volumes were 0.029 and 0.168 ml, as measured from the autosampler to the DAD detector or to the RF detector cell, respectively. All the retention data were corrected for these contributions.

3.2. Chemicals

The organic components of the mobile phases, HPLC grade methanol and acetic acid, were purchased from Fisher Scientific (Fair Lawn, NJ, USA). Water was purified with a Barnstedt E-pure system from Thermo Fisher Scientific (Waltham, MA, USA). Sodium acetate was for molecular biology grade from Sigma–Aldrich (St. Louis, MO, USA). Dichloromethane (ACS grade) required to perform pycnometric measurements was also obtained from Fisher Scientific. Deuterated methanol (99.8%) used for hold-up volume and adsorption measurements was from Alfa Aesar (Ward Hill, MA, USA). $NaNO_3$ (AR grade) used as a non-retained tracer was from Mallinckrodt (Paris, KY, USA).

3.3. Columns

We used two identical 250 mm × 4.6 mm columns coming from the same batch, packed with ~2.5 g of (*S*,*S*)-Whelk-O1 non-endcapped material, 5 μm particle size, 100 Å pore size, spherical silica (Regis Technologies, Morton Grove, IL, USA). The surface area of the silica is 200 m^2/g and its internal porosity 0.5 cm^3/g as reported by the manufacturer. Before experiments, both columns were flushed with 200 ml of isopropanol and 200 ml methanol followed by conditioning in the working mobile phase during not less than 1 h at a flow rate of 1 ml/min.

The first column (serial number 400694) was used for the measurement of the excess adsorption isotherm in water–methanol mixtures, of the hold-up volume by different methods, and for reliability tests described below (column 1 hereinafter). The experiments on the adsorption of Naproxen enantiomers were carried out with the second column with serial number 100702 (column 2 hereinafter).

3.4. Procedures

3.4.1. Excess adsorption from binary mixtures methanol–water

The excess adsorption isotherms of methanol and water were determined by means of the minor perturbation method described in detail in [25,30]. The measurements were carried out at 34.7 °C. The flow rate was kept at 1 ml/min. The column was successively equilibrated with a mobile phase containing 0, 0.5, 1, 5, 10, 20, 30, 40, 50, 60, 70, 80, 90, 95, 99, 99.5 and 100% volume of water. Methanol–water mixtures were prepared by the volumetric method, using measuring cylinders of appropriate sizes, unless the volume required was less than 5 ml, in which case volumetric pipettes were used. Conversion from volume fractions to molar concentrations was made based on the values of the densities of pure water [31], methanol [32] and of methanol–water mixtures [32]. The minor perturbation of the equilibrium between the liquid and the stationary phase was caused by the injections of 2 μl of one of two types of solutions, in which there was a 5–10% excess of either water or methanol over the mobile phase composition. Retention times of these positive and negative perturbations were averaged and the averaged data used for the calculation of the excess adsorption isotherm, according to the following equation [25] is:

$$\Gamma_i(c_{e,i}) = \frac{1}{V_a}\int_0^{c_{e,i}} (V_R(c_{e,i}) - V_0)\,\mathrm{d}c_{e,i} \tag{7}$$

where $V_R(c_{e,i})$ is the retention volume of the perturbation peak on the plateau of concentration $c_{e,i}$ of a component i and V_0 is the column hold-up volume. The correction for thermal expansion of the mobile phase from the ambient temperature in the pump (T_0) to the column temperature (T_{col}) was taken into account by multiplying the volume values and dividing the concentration values by the ratio of the mobile phase densities at temperatures T_0 and T_{col}, respectively.

3.4.2. Measurement of the hold-up volume

The accurate determination of the hold-up volume is essential for the correct measurement of adsorption isotherms [33]. There are different definitions of this quantity [30,34,35]. In this work, we use an operational definition that is consistent with Eq. (1) and considers the hold-up volume as the volume of the column that is accessible to the mobile phase. Three methods were employed to evaluate V_0: the minor perturbation, the pycnometry, and the isotopic methods:

(a) *Minor perturbation method*. The estimate of the hold-up volume by the minor perturbation method was carried out based on the experimental data obtained in measuring the excess adsorption isotherms described in the previous section. The V_0 value was determined by integration of the dependence of $V_R(c_i)$ through the entire concentration range of either component of the binary mobile phase (where $c_i^\star$ is the molar concentration corresponding to the pure solvent i) as [30]:

$$V_0 = \int_0^{c_i^\star} V_{R,i}(c_i)\,\mathrm{d}c_i \tag{8}$$

This value was used in the calculations made with Eq. (7).

(b) *Pycnometry method*. The pycnometry method [34] yields the hold-up volume from the weights of the column when filled with two different pure liquids of substantially different densities. The pycnometry measurements were performed with pure methanol and dichloromethane at ambient temperature (20 °C) following the experimental protocol given in [35].

(c) *Isotopic method*. Measurements were made with an isotopically labeled solute, at temperatures of 34.7, 40, 47.1 and 57.1 °C using pure methanol as the mobile phase and deuterated methanol as the tracer. The tracer concentration was 1 vol.%, and the sample size was 2 μl. The retention volume of labeled methanol is equal to V_0 by definition [34].

3.4.3. Investigations of water–acetic acid mixtures

The elution of acetic acid with pure water was studied at 34.7 °C, using injections of 2 μl of the acid solutions, with concentrations ranging from 0.18 to 3.49 M.

Frontal analysis measurements were made with aqueous solutions of acetic acid as the mobile phase, at temperatures of 22, 34.7, 40, 47.1, and 57.1 °C. The acid concentration in the mobile phase was increased stepwise from 0 to 0.053 M with 10% steps. The column was conditioned at each concentration step for no less than 0.5 h, followed by an injection of 2 μl of acetic acid solution to induce a minor perturbation on the concentration plateau. These

Table 1
pH of the mobile phases and dissociation constants of Naproxen.

Mobile phase	${}^{s}_{w}$pH	δ [a]	${}^{s}_{s}$pH	${}^{s}_{s}pK_a$ [b]
Pure buffer [c]	4.21			4.40 [d]
MeOH–buffer (60:40, v/v)	5.35	0.176	5.17	5.78
MeOH–buffer (70:30, v/v)	5.67	0.176	5.49	6.19
MeOH–buffer (80:20, v/v)	5.91	0.045	5.86	6.58

[a] Ref. [37].
[b] Ref. [57].
[c] 0.09 M CH_3COOH + 0.03 M CH_3COONa.
[d] In pure water.

experiments were found to damage the stationary phase. Therefore their results are discussed here only as far as they concern the stability of the stationary phase.

3.4.4. Adsorption of the Naproxen enantiomers from methanol–water buffer mixtures

3.4.4.1. Mobile phases. The solvents used to investigate the adsorption of Naproxen were mixtures of methanol and acetic buffer solution in the ratio 60:40, 70:30, and 80:20 (v/v). The buffer solution contained 0.09 M CH_3COOH + 0.03 M CH_3COONa, and was filtrated through 0.45 μm type FH membranes (Millipore, Bedford, MA, USA). After mixing, the mobile phases were degassed by ultrasonication, followed by the measurement of the pH with the American pH II pH-meter (Baxter Scientific, Stone Mountain, GA), calibrated against aqueous standard buffers. The pH value obtained, ${}^{s}_{w}$pH, relates to the pH value expressed in a scale for the given mixed solvent, ${}^{s}_{s}$pH as [36]:

$$ {}^{s}_{s}\mathrm{pH} = {}^{s}_{w}\mathrm{pH} - \delta \tag{9} $$

The δ parameter is a constant for a given electrode system in a certain solvent [37]. Table 1 lists the measured values of ${}^{s}_{w}$pH and the calculated values of ${}^{s}_{s}$pH as a function of the mobile phase composition. In these calculations the δ values determined with the glass electrode in methanol–water solutions reported by Canals et al. [37] were used.

3.4.4.2. Calibration of the detector response. All the experiments requiring conversion of the detector signal to a concentration scale were carried out under conditions of linear detector response. This was achieved by selecting an appropriate DAD detector wavelength. Then the concentration relates to the detector response h as follows

$$ c = rh \tag{10} $$

The detector response factor r is found from the chromatogram to be converted by means of the following expression:

$$ r = \frac{m}{SF} \tag{11} $$

where m is the amount of solute injected, S is the peak area, and F is the flow rate. In the calculations, the value of the detector response factor averaged over a series of chromatograms was used.

3.4.4.3. Determination of the adsorption isotherms by the pulse method. The adsorption equilibrium of the Naproxen enantiomers was measured by a modified Glueckauf method [38,39], in which sample pulses of increasing sizes are injected, after the column had been equilibrated with the mobile phase. To derive the adsorption isotherm, the following equation was applied:

$$ \frac{\mathrm{d}q(c)}{\mathrm{d}c} = \frac{(V_R(c) - V_0)}{V_a} = V'_R(c) \tag{12} $$

where $V_R(c)$ is the retention volume of the apex of the peak corresponding to the mobile phase concentration of an adsorbate at the apex, and $q(c)$ being the adsorbed amount of solute at equilibrium with this concentration c. Thus, the retention time of each peak gives one point on the $V'_R(c)$ versus c plot. By repeating the procedure while progressively increasing the concentration of the sample, the set of data $V'_R(c)$ versus c is obtained within the concentration range of interest. The amount adsorbed $q(c)$ is obtained by integration of the area under the function $\mathrm{d}q(c)/\mathrm{d}c$ from 0 to c.

The measurements were carried out at 34.7 °C at a flow rate of 1 ml/min. The sample volume was 20 μl, and the sample concentration was increased from 0.07 to 34.89 mM. The achievement of equilibrium conditions was verified by checking that the dispersed rear boundaries of the peaks obtained for different sample sizes overlay. In the rare cases in which this condition failed, the whole series of measurements for both enantiomers were repeated till the condition was fulfilled. Since gradual deterioration of the stationary phase in the first column was found under the experimental conditions discussed below, it is important to note that all the experiments discussed here were performed with the "fresh" column 2, during the first 2 days of its service.

3.4.4.4. Determination of the adsorption isotherms by the inverse method. The inverse method provides the numerical coefficients of a preset isotherm model through an optimization procedure that minimizes the distance between an experimental overloaded band profile and the profile calculated with a suitable model of chromatography [40]. The equilibrium-dispersive (ED) model of chromatography [40] was used in the present calculations. The mass balance equation for this model is

$$ \frac{\partial c_i(z,t)}{\partial t} + \left(\frac{1-\epsilon}{\epsilon}\right)\frac{\partial q_i(z,t)}{\partial t} + u\frac{\partial c_i(z,t)}{\partial z} = D_a\frac{\partial^2 c_i(z,t)}{\partial z^2} \tag{13} $$

where z is the abscissa along the column, t the time, u the mobile phase linear velocity, and ϵ the total porosity of the column. D_a is the apparent axial dispersion coefficient. It relates to the theoretical plate number N and the column length L through the equation:

$$ D_a = \frac{Lu}{2N} \tag{14} $$

The plate number of the column must be measured under linear conditions, i.e., with sample sizes that are so small that the efficiency is independent of the sample size.

The calculation of a numerical solution of a partial differential equation requires initial and boundary conditions. The following conditions are used to solve Eq. (13):

- The initial conditions are $c_i(z,0) = 0$ and $q_i(z,0) = 0$. They state that at $t = 0$, the column is in equilibrium with the pure mobile phase.
- The boundary condition at the column inlet (at $t > 0$ and $z = 0$) is defined by the injection of a rectangular plug of solution:

$$ c_i(0,t) = \begin{cases} c_i^0 & \text{if } 0 < t < t_p \\ 0 & \text{if } t_p < t \end{cases} \tag{15} $$

  where t_p is the duration of the injection and the superscript 0 indicates an "inlet value".
- The boundary condition at the column outlet (at $t > 0$ and $z = L$) is

$$ \frac{\partial c_i}{\partial z} = 0 \tag{16} $$

The mass balance equation supplemented with a proper isotherm model and the initial and the boundary conditions was integrated numerically by orthogonal collocation on fixed finite elements [41]. The optimization procedure used to find the best fitting isotherm parameters [42] was performed on the elution profiles obtained during pulse experiments with samples of the highest

Table 2
Comparison of column performance characteristic as reported by the manufacturer and measured after a period of exploitation [a].

	Column 1		Column 2	
	k'_1 [b]	α	k'_1 [b]	α
Manufacturer	1.80	3.80	2.29	3.45
After use	0.25	1.93	2.16	3.24

[a] Mobile phase: hexane–isopropanol, 90:10 (v/v); flow rate: 1 ml/min.
[b] The retention factor of the less retained enantiomer.

sample concentration studied (34.89 mM). The optimization algorithm was one of Marquardt, modified by Fletcher [43].

4. Results and discussion

4.1. Adsorbent stability under reversed-phase conditions

Several scientists used the Whelk-O1 CSP with water containing mobile phases modified by addition of an acid or a base [10,17,19–22]. They also ran it at temperatures up to 50 °C [21]. According to the manufacturer specifications, this column can be used at any pH between 2.5 and 7. Therefore, we did not expect any significant deterioration of the CSP with solutions of acetic acid in the pH range just mentioned, at least during a short period of time. However, we observed a poor reproducibility of the frontal analysis data obtained with the first column when using aqueous acetic acid solutions at pH ≥ 3 and at temperatures higher than 40 °C. The highest temperature to which the column was exposed during 1 day was 57 °C. When this series of experiments was ended, a chromatogram of *rac-trans*-stilbene oxide was recorded under standard conditions, revealing a major decrease of the retention times and of the separation ability (Table 2). Comparison of the hold-up volumes of the column determined before and after this series of measurements showed an increase of 5%, suggesting a certain degree of destruction of the packing material. It is also worth noting that when the column was flushed with methanol after the series of high temperature frontal analysis experiments, we observed the elution of a turbid yellow liquid, suggesting the release of organic or silica-organic species (a product of hydrolysis at the Si–O bond, see Fig. 1) including the chiral selector, which has a yellow color [44].

The second column was exposed to milder conditions. It was eluted with methanol–acetic buffer mixtures (Table 1) at temperatures no higher than 34.7 °C. Nevertheless a progressive, if slower deterioration of the column performance was also observed. A sudden change of the retention times and selectivity of the Naproxen enantiomers was observed after a (quasi)equilibrium state had been achieved, as illustrated in Fig. 2. The new equilibrium state was always characterized by a slightly lower retention than the previous one. This situation is illustrated in Fig. 2 by a series of chromatograms of *rac*-Naproxen obtained during a period of 6 h, with the same mobile phase. At the end of a 1-week period of exploitation of the column 2, a chromatogram test of *rac-trans*-stilbene oxide was recorded. It showed minor changes from the test chromatogram provided by the manufacturer (Table 2). Thus, the CSP under study does not tolerate aqueous acidic solutions at elevated temperatures and is not stable in weakly acidic methanol–water buffer solutions, although in the latter case little damage was done to the column. All the experimental results discussed below were obtained during the initial period of exploitation of the two columns, when the deterioration of their performance was still moderate. These results illustrate the properties of Whelk-O1 CSP at its maximal retention capacity.

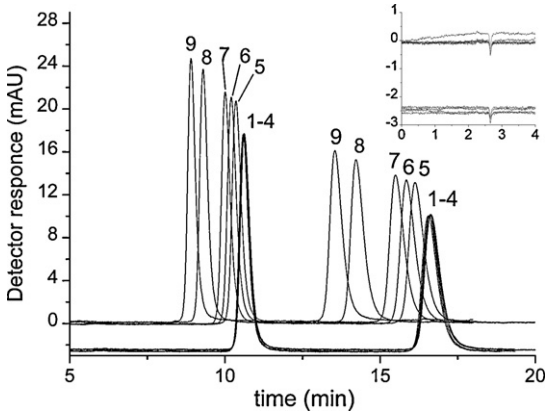

Fig. 2. Series of chromatograms of racemic Naproxen after sequential injections. The numbers above the peaks refer to the injection number. The time interval between injections was 10–20 min. Before the first injection the column was equilibrated with the mobile phase for 1 h. Peaks 1–4 demonstrate that a quasi-equilibrium state takes place. The inset shows an initial part of the chromatograms including the injection perturbation. Note that its retention time does not change, proving that the drift of the Naproxen retention is not caused by a fluctuation of the flow rate or of any process affecting the hold-up volume.

4.2. Hold-up volume

The values of the hold-up volume determined by different methods are compared in Fig. 3. The results obtained by the minor perturbation and the isotopic methods agree well together whereas the pycnometry method yields a somewhat overestimated value compared to those provided by the other two methods. This difference can be ascribed to experimental errors made in applying the pycnometry method, which involves several manual procedures, like retrieval of the column from the chromatograph and drying the column endfittings [35].

The isotopic method data corrected for the solvent thermal expansion show a slight increase of the hold-up volume with increasing temperature while the uncorrected results decrease, exhibiting a larger slope. This shows that a significant part of the temperature dependence of the hold-up volume is accounted for by the thermal expansion of the mobile phase. This same dependence is found in values derived from measurements of the retention time of $NaNO_3$ eluted with the methanol–acetic buffer mobile

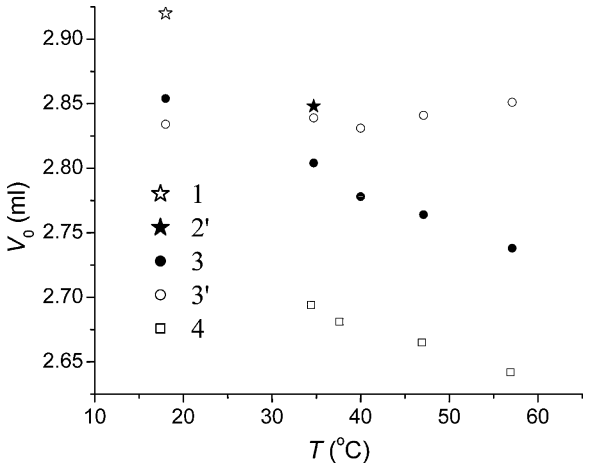

Fig. 3. Evaluation of the hold-up volume by different methods at different temperatures: (1) pycnometry method, (2) minor perturbation method, (3) isotopic method, and (4) retention of $NaNO_3$ from the mobile phase MeOH–acetic buffer (80:20, v/v). Symbol "prime" refers to results corrected for thermal expansion of the mobile phase.

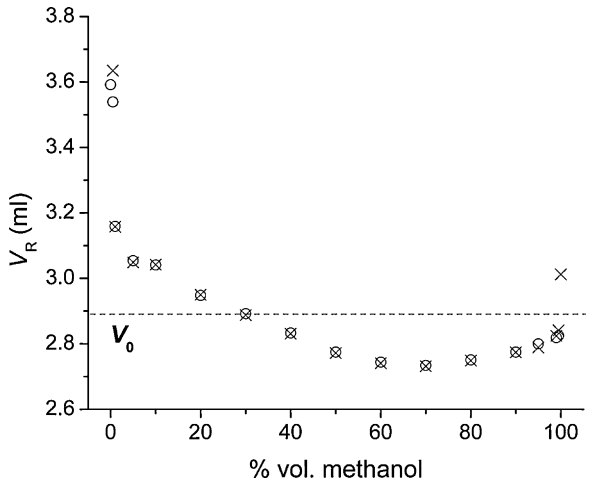

Fig. 4. Dependence of the retention of the minor perturbation peaks of methanol (circles) and water (crosses) from methanol–water solutions on the methanol volume fraction.

phase (see Fig. 3). Note that the hold-up volume derived from the retention volume of sodium nitrate is lower by 0.458 ml than the one derived from the retention time of deuterated methanol. Evidently, the nitrate anion is expelled from the adsorbed layer, due to electrostatic repulsion between the anion and the electronegative aromatic moieties of the bonded organic phase. An estimate of the size of this "expulsion zone" gives a thickness of ~9 Å, about 3 times the dimension of the solvent molecules (methanol and water), suggesting that the layer inaccessible to the nitrate anions is not uniformly thick. Possibly, it fills the space between the bonded chiral selectors and the silica surface, a volume which becomes accessible to the mobile phase components but not to the anion species.

4.3. Adsorption of methanol–water mixture

Fig. 4 shows a plot of the reduced retention volume derived from the retention times of water and methanol perturbations versus the mobile phase composition. There is an excellent agreement between the two series of data, except at the extreme regions of the plot, although even there the discrepancy between them is small. The corresponding excess adsorption isotherms are given in Fig. 5, showing that the adsorption of methanol is positive and that of water negative through the entire range of solution composition. Thus, the grafted organic layer is relatively hydrophobic, expelling water in the presence of methanol, which can be accounted for by the influence of the large phenanthryl fragment of the chiral selector (see Fig. 1). However, it must be noted that a negative excess adsorption does not mean complete exclusion of water from the adsorbed layer but indicates a decrease of its concentration compared to that in the bulk phase. The isotherm of total adsorption (Fig. 5) evinces the presence of water in the stationary phase while there is water in the mobile phase. These isotherms were calculated using Eq. (2) with the τ value determined after [25], based on an earlier work of Everett [45]. According to this method, τ is derived from the slope of the linear part of the excess adsorption isotherm of the preferentially adsorbed component. This result gives a thickness of 2.12 Å for the adsorbed layer of methanol, which indicates the monolayer character of its adsorption on the surface of Whelk-O1. The same value was found for the adsorption of methanol from aqueous solutions on different reversed-phase adsorbents [25,46].

Consideration of the total adsorption isotherms suggests that complete filling of the adsorption layer by methanol (~5 molecules per chiral selector) is achieved for a bulk phase composition of

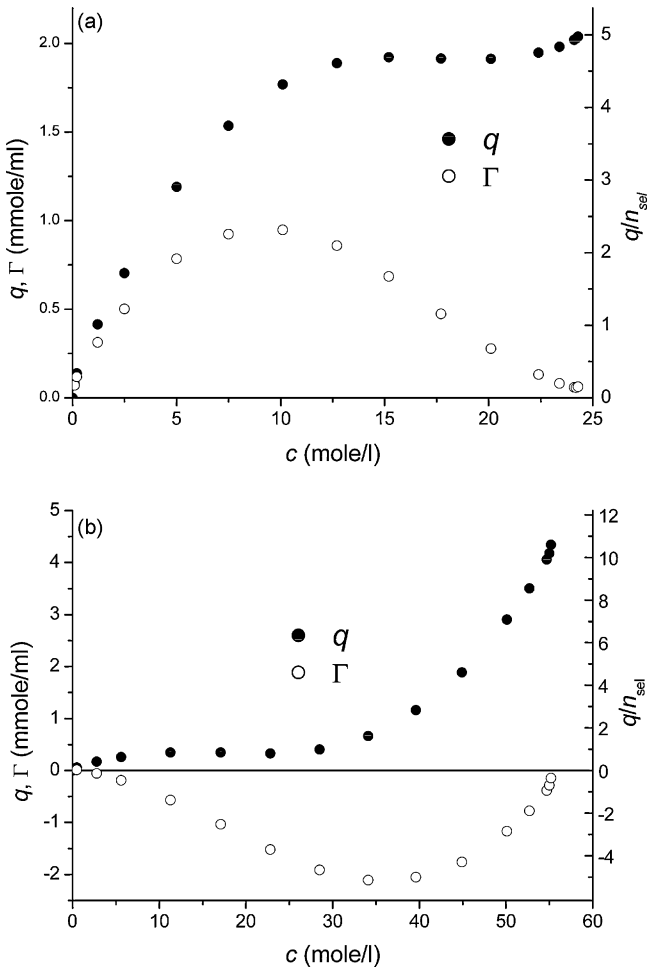

Fig. 5. Total and excess adsorption isotherms of methanol (a) and water (b) at 34.7 °C. The right ordinate axis shows the number of solvent molecules per chiral selector (n_{sel} is the concentration of chiral selectors).

~50% water (v/v). When the water fraction of the mobile phase increases, its concentration in the adsorption layer, which is low below that point (less than 1 molecule per chiral selector group), steeply increases and approaches a value of 10.6 molecules per chiral selector.

4.4. Retention of acetic acid

The retention of eluent additives on the stationary phase is usually not taken directly into account in adsorption models. At the same time, if the adsorption coefficient of an additive is comparable to that of a solute, a dramatic distortion of this solute elution profile may be observed [47–49]. Therefore, it is important to estimate the adsorption coefficient of acetic acid. Fig. 6 shows the elution profiles of increasing amounts of acetic acid. When the sample size is small, hence its dissociation degree large, acetic acid elutes earlier than the mobile phase itself because the acetic anion is expelled from the adsorbed layer, like the nitrate anion. Note that the acetic acid peaks are anti-Langmuirian at low concentrations. Increasing the sample concentration results in a shift of the retention time beyond the hold-up time. Besides, at high concentrations, the peak shape tends to be Langmuirian and, in both cases, fronting extends behind the hold-up time. This is obviously consistent with the increasing fraction of the neutral form of the acid in the elution band. In spite of the positive retention of the undissociated acid, it remains negligible and cannot interfere with the elution of Naproxen.

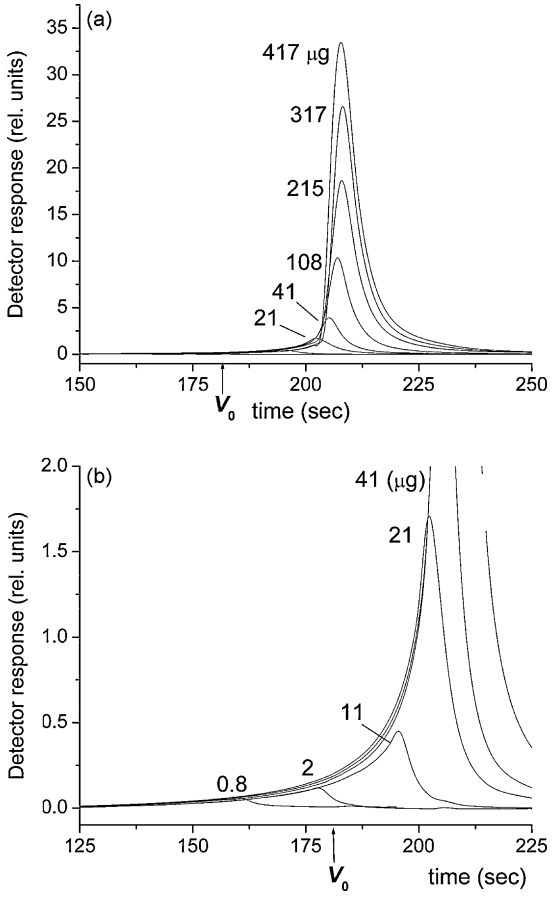

Fig. 6. Illustration of the effect of the sample size on the retention and shape of the elution profile of acetic acid. Sample volume 2 μl; flow rate 1 ml/min. The injected amounts of acid are shown next to the respective profiles. Part (a) shows all the chromatograms, and part (b) shows the chromatograms for injected amounts between 0.8 and 21 μg in an expanded scale.

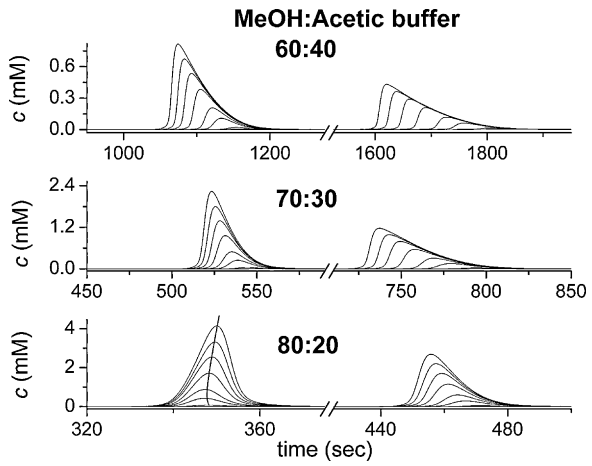

Fig. 7. Illustration of the effect of the mobile phase composition and the sample size on the elution profiles of naproxen enantiomers ((*R*) is the first eluted enantiomer). Sample volume 20 μl; sample concentrations: 0.07, 0.17, 0.70, 3.5, 13.6, 20.9, 27.9, and 34.9 mM.

4.5. Adsorption of Naproxen

4.5.1. General considerations

Whelk-O1 CSP was developed for the resolution of Naproxen enantiomers and is characterized by its high enantioselectivity towards them under normal-phase conditions. The same selectivity is observed in the reversed-phase mode, the selectivity coefficient ranging between 1.76 and 1.70 for mobile phase compositions between 60:40 and 80:20 (methanol–acetic buffer, v/v) at 34.7 °C. The large distance between the two enantiomer peaks suggests a low density of nonselective sites on the surface of the CSP. A closer examination of the peak shapes reveals a relatively long tailing for both enantiomers (Fig. 7), a tailing too strong to be accounted for by the Langmuir isotherm, as confirmed by numerical calculations (not reported here). A possible explanation would be that this tailing results from the strong interaction of Naproxen with the nonselective sites. These sites can belong to areas of the support surface uncovered by chiral selectors. Organically modified silica is known to bear free silanol groups responsible for the strong retention of polar solutes. The density of these adsorption sites is small [50] and the effective surface concentration must be still smaller due to the shielding effect of the grafted organic layer. This could be consistent with the assumption of the existence of a low density of strong, nonchiral adsorption sites.

The most intriguing finding of this study is the evolution of the overloaded band profiles of the less retained enantiomer ((*R*)-Naproxen) from Langmuirian to anti-Langmuirian shape when the methanol content in the eluent increases (Fig. 7). This means that the adsorption mechanisms for (*R*)- and (*S*)-Naproxen are fundamentally distinct, which cannot be explained in the framework of simple two-site models. Besides, the adsorption model for (*R*)-Naproxen has to depend on the methanol–acetic buffer ratio in a way that would allow an evolution of a peak shape corresponding to the evolution of the adsorption isotherm, from convex to concave.

The enantiodiscrimination of the Naproxen enantiomers requires simultaneous interactions between the three functionalities of (*S*)-Naproxen (i.e., the aryl residual, the hydroxyl group, and the carboxylate oxygen) and the complimentary parts of the selector moiety [3]. Similar interactions are likely to be sterically hindered in the case of the less retained (*R*)-Naproxen. Therefore a functionality or functionalities of this enantiomer uninvolved in the stereoselective interaction with Whelk-O1 selector is able to form an adsorbed homochiral dimer with another analyte molecule from the bulk solution. Then the total adsorption mechanism can be described by the following schemes where the symbols S and R stand for (*S*)- and (*R*)-enantiomers, and the symbols Ch and NCh for the chiral selectors and the nonchiral adsorption sites, respectively. The symbols of the respective equilibrium constants are given on the right of the equations.

- For (*S*)-naproxen:

$$\mathrm{S} + \mathrm{Ch} \rightleftharpoons \mathrm{S\text{-}Ch}, b_S \tag{17}$$

$$\mathrm{S} + \mathrm{NCh} \rightleftharpoons \mathrm{S\text{-}NCh}, b_{ns} \tag{18}$$

- For (*R*)-naproxen:

$$\mathrm{R} + \mathrm{Ch} \rightleftharpoons \mathrm{R\text{-}Ch}, b_R \tag{19}$$

$$\mathrm{R} + \mathrm{R\text{-}Ch} \rightleftharpoons \mathrm{R_2\text{-}Ch}, K_{dim} \tag{20}$$

$$\mathrm{R} + \mathrm{NCh} \rightleftharpoons \mathrm{R\text{-}NCh}, b_{ns} \tag{21}$$

The corresponding adsorption isotherms are

- For (*S*)-naproxen:

$$q = \frac{q_{ns}^{\star} b_{ns} c}{1 + b_{ns} c} + \frac{q_S^{\star} b_S c}{1 + b_S c} \tag{22}$$

• For (*R*)-naproxen:

$$q = \frac{q_{ns}^{\star} b_{ns} c}{1 + b_{ns} c} + \frac{q_S^{\star} b_R c}{1 + b_R c - 2K_{dim} c/(1 + 2K_{dim} c) - b_R K_{dim} c^2/(1 + 2K_{dim} c)} \quad (23)$$

Eq. (23) can describe either a Langmuir-type or an S-shape isotherm, depending on the numerical values of its parameters. If the contribution of the nonselective adsorption sites can be neglected, the condition $b_R > 2K_{dim}$ defines a field of convex isotherms and the converse inequality a field of S-shape isotherms, provided that the quadratic term of the denominator of the selective adsorption term is negligible. This latter approximation is reasonable since the quadratic term accounts for less than 1% of the denominator within the range of concentrations investigated.

It is important to discuss one more approximation of the model considered. Naproxen exists in the mobile phase as two species in equilibrium, a neutral acid and a basic anion. When the mobile phase contains a sufficiently large concentration of the buffer, the hydrogen-ion concentration can be assumed to be constant during the whole elution process so the degree of dissociation (α) is constant too. Calculation gives α values of 0.23, 0.19, and 0.19 for methanol fractions in the mobile phase of 60, 70, and 80% (v/v) (details of the calculation are given in Appendix A). Since the methanol concentration is higher in the adsorbed than in the bulk phase, the percentage of anions in contact with chiral selectors should be lower there than in the eluent. From experimental and theoretical studies of the chromatography of weak acids on bonded phases [51,52], we know that a convenient adsorption model in such systems is the sum of two Langmuir terms for each kind of species, the concentrations of these species being expressed as the product of the total concentration of the acid and the dissociation degree, $c\alpha$ and $c(1-\alpha)$ of the neutral and ionized forms, respectively. The following circumstances should be taken into account:

(1) The influence of the methanol concentration on α within the range investigated is insignificant, therefore it cannot explain the effect of the mobile phase composition on the adsorption.
(2) The lack of a diffuse elution front suggests that the Naproxen anion is not repulsed as the acetate anion, due to the attractive π–π interactions between the aryl radical of Naproxen and the aromatic system of the Whelk-O1 moiety. Besides the negative charge of the Naproxen anion is delocalized due to its conjugation with the π-electron system of the naphthyl radical. Therefore, its repulsion from the hydrophobic parts of the chiral selectors is weaker than for small size anions (e.g., NO_3^-).
(3) Anions adsorb on the same chiral sites as neutral acids but with a somewhat smaller adsorption coefficient due to the repulsive interaction between the anions and the hydrophobic groups of the chiral selector. Since the concentration of these sites is large compared to the solute concentration, the respective Langmuir terms can be approximated by linear (Henry) terms. Designating the adsorption coefficients for the dissociated ion and the neutral acid as b_A and b_{HA}, respectively, one can write

$$q_S^{\star} b_{HA} c(1-\alpha) + q_S^{\star} b_A c\alpha = q_S^{\star} c[b_{HA} + \alpha(b_A - b_{HA})] = q_S^{\star} c b_{app} \quad (24)$$

It is impossible to separate the contributions of the anionic and the neutral forms of Naproxen to its adsorption if their local isotherms are close to linear. Moreover, since $\alpha \approx 0.2$ and $b_{HA} > |b_A - b_{HA}|$ then $b_{app} \approx b_{HA}$.

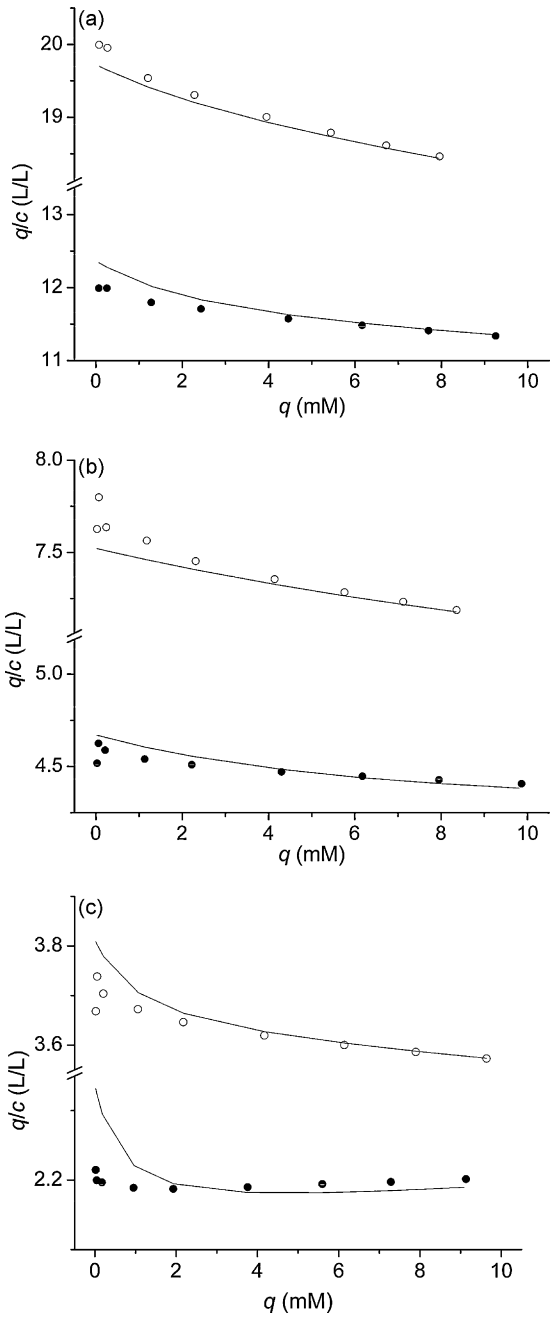

Fig. 8. Adsorption isotherms of (*R*)-Naproxen (full circles) and (*S*)-Naproxen (empty circles) determined by the pulse method (circles) and by the inverse method (lines).

The situation is different for adsorption on the nonselective sites. Their concentration is close to that of the solutes. Consequently, the local isotherms for these adsorption sites behave in a strongly nonlinear way. On the other hand, the contributions of the nonselective retention sites is minor compared to that of the selective sites. Therefore the separation of the effects from the neutral and the ionic nonselective adsorption sites is a statistical task that is beyond the precision of the collected data. Thus, the adsorption models in Eqs. (22) and (23), which does not include separate terms describing the adsorption of dissociated Naproxen species, will be used to analyze the experimental results.

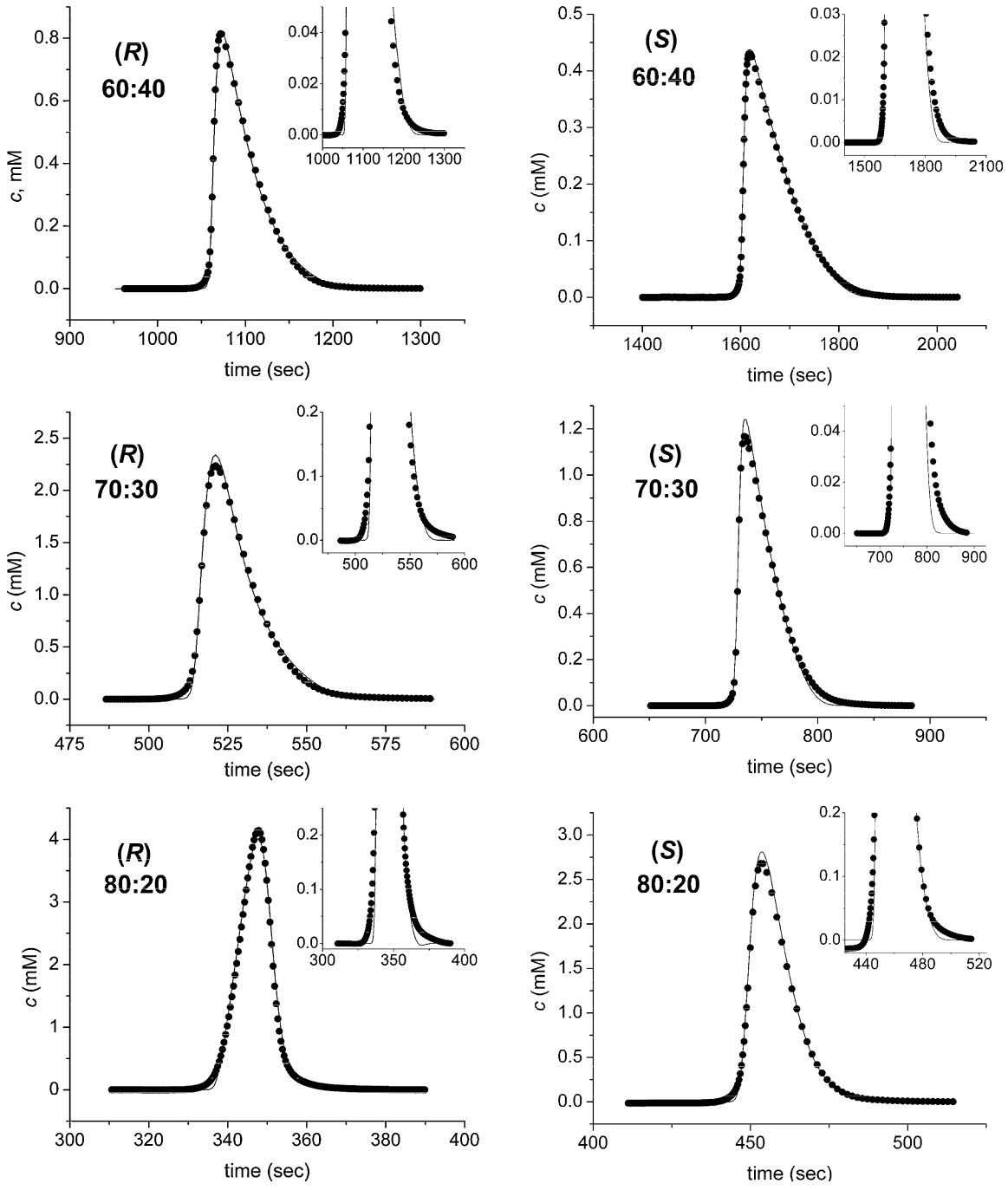

Fig. 9. Comparison of the experimental and calculated elution profiles of (*R*)-Naproxen (left column) and (*S*)-Naproxen (right column). Sample volume 20 μl; concentration 34.9 mM. Insets show the low concentration part of the elution profiles in an expanded scale.

4.6. Pulse method

The Glueckauf method can be applied to derive the adsorption isotherms from the retention volume data only if equilibrium is proven. A good indication of instantaneous equilibrium in a column is the fact that the dispersed fronts belonging to different sample sizes nearly coincide [53]. Fig. 7 demonstrates that this takes place in all cases, except for (*R*)-Naproxen at 80% methanol (v/v) for which the elution profiles of small size samples do not approach neither flanks of the profiles of larger size samples. Obviously, this is because the size of these samples is in a range such that a slightly convex isotherm turns into a concave isotherm as the sample size increases. A line drawn through the maxima of the peaks in the series shows a trend in retention times, which decrease with increasing size for small size samples then begin to increase with increasing sample size for more concentrated samples (Fig. 7). The respective equilibrium isotherms are shown in Fig. 8, in Scatchard plot coordinates. The adsorption systems are non-Langmuirian. The isotherm of (*R*)-Naproxen evolves from one that is close to Langmuirian to one that is strictly bi-Langmuirian, and to one that cannot be a bi-Langmuirian isotherm when the methanol concentration increases. The approximation of the experimental isotherms with the models in Eqs. (22) and (23) results in a good agreement between the fitted and the experimental data. At the same time, the best fit coefficients depend strongly on the initial guess values involved in the fitting algorithm, which is due

Table 3
The best fit isotherm coefficients and their standard deviations (in parenthesis) obtained by the inverse method.

Coefficient	Methanol–acetic buffer ratio (v/v)		
	60:40	70:30	80:20
q_{ns} (mM)	0.220 (0.004)	1.230 (0.005)	0.057 (0.003)
b_{ns} (mM^{-1})	4.49 (0.07)	0.51 (0.02)	3.50 (0.08)
q_s (mM)	231 (1)	494 (11)	600 (4)
b_S (mM^{-1})	0.0813 (0.0004)	0.0140 (0.0004)	0.0060 (0.00002)
b_R (mM^{-1})	0.0494 (0.0002)	0.0082 (0.0002)	0.0036 (0.00003)
k_{dim} (mM^{-1})	0.0115 (0.0002)	0.0069 (0.0002)	0.0041 (0.00005)
$q_{ns}b_{ns}$	0.99	0.63	0.20
q_sb_R	11.38	4.04	2.14
q_sb_S	18.74	6.89	3.61
$2K_{dim}/b_R$	0.47	1.69	2.29
N_R	5000	6500	7400
N_S	4500	5500	7400

to the weak degree of nonlinear behavior of the isotherms (data not shown). The inverse method provides an alternative possibility to evaluate the isotherm parameters. Because the shape of an elution profile is sensitive to variations in the values of the isotherm coefficients, one can expect that this method will give more robust estimates of those.

4.7. Inverse method

Fig. 9 compares experimental chromatograms and elution profiles calculated with the isotherm parameters and the plate numbers provided by the inverse method (Table 3). Since the adsorption models for (*S*)- and (*R*)-Naproxen have common coefficients ($q^{\star}_{ns}$, $q^{\star}_{s}$, and b_{ns}), the model parameters were determined by the simultaneous fit of the chromatograms of both enantiomers, in order to decrease the number of independent adjustable parameters. The figure shows an excellent coincidence of experimental and calculated profiles. Small discrepancies are only found in the diffuse boundaries, whether at the front or rear of the bases of the elution profiles. These fronting and tailing do not originate from a dispersion of the injection profiles because the calculations of band profiles made with either recorded injection profiles or rectangular pulses as initial conditions showed the same dispersion effect (not reported data). Thus, these differences in the peak profiles suggest that some minor unaccounted contributions to the retention mechanisms remain. The adsorption isotherms calculated from the coefficients in Table 3 are plotted in Fig. 8. The curves are in a good agreement with the equilibrium data measured by the pulse method but a visible divergence in the low adsorption region is apparent. It is due to the low value of the bulk concentration of the adsorbate that figures in the denominator. In fact, this discrepancy accounts for less than 5% of q.

Considering the data in Table 3, the following regularities can be observed:

(1) The total retention of both enantiomers decreases with increasing methanol concentration of the mobile phase, with the contributions of both the nonselective and the selective terms (products $q^{\star}_{ns}b_{ns}$ and $q^{\star}_{s}b_{s}$, respectively) declining.
(2) The nonselective adsorption sites are the high-energy sites; their adsorption constants are two to three orders of magnitude larger than those of the selective sites; the concentration of the nonselective sites is two to four orders of magnitude smaller than that of the selective sites.
(3) The concentration of the selective adsorption sites increases and their adsorption constant decreases with increasing methanol concentrations in the mobile phase.
(4) The K_{dim} constant decreases but the ratio $2K_{dim}/b_R$ increases with increasing methanol concentration.

The first observation demonstrates the influence of the solvation ability of the mobile phase on the adsorption of Naproxen. Note that methanol solvates Naproxen better than water, as shown by a comparison of the standard Gibbs energies of solvation of Naproxen in methanol and water, −47 kJ/mol [54] and −24 kJ/mol [55], respectively. Therefore, the higher the methanol fraction in the mobile phase, the larger the organic solute fraction that is extracted by the solvent from the surface layer.

The second observation is consistent with the assumption that the nonselective sites are residual silanol groups on the silica surface. Their contributions to the total retention is minor, accounting for less than 14% of the Henry coefficient for the less retained enantiomer. The third observation is that the effect of the methanol/acetic buffer ratio on the behavior of the selective adsorption sites affects not only the equilibrium constants but also the saturation capacities. The former can be ascribed to the influence of the solvation ability of the eluent already mentioned. The latter fact has no clear explanation. It is unlikely to be connected directly to the change in methanol/water ratio. Within the range of mobile phase compositions studied, the concentrations of water and methanol in the adsorbed layer hardly change. Therefore, whatever the composition of the bulk solution, the proportions of methanol and water in the solvate sphere of the chiral selectors must be the same. Rather the effective concentration of the enantioselective sites is affected by the presence of buffer additives, acetic acid and sodium acetate. Indeed, a increase of $q^{\star}_{s}$ correlates with a decrease of the buffer system concentration in the mobile phase.

The change in the ratio $2K_{dim}/b_R$ accounts for the evolution of the shape of the adsorption isotherms and, consequently, of the shape of the (*R*)-Naproxen band profiles. Two simplifications must be made to allow a qualitative analysis of the isotherm in Eq. (23) in order to clarify the effect of this ratio. First, we must omit from consideration the nonselective term of the isotherm. Second, we must neglect the contribution of the quadratic term of the denominator of the second term of the isotherm, which is minor within the concentration range studied. Then it can be shown that the inflection point of the isotherm in Eq. (23) is located at the origin of the q versus c coordinate system, if the ratio of interest is equal to 1. Increasing this ratio beyond 1 results in a shift of the abscissa of the inflection point towards positive values. Then, the isotherm becomes concave upward between zero and the inflection point. If, however, the contribution of nonselective adsorption is not negligible, the critical value of the ratio $2K_{dim}/b_R$ shifts upwards from 1. This explains why one observes a convex isotherm for a mobile phase composition of 70:30 (v/v), for which $2K_{dim}/b_R = 1.69$.

It is interesting to note that, in spite of the relative importance of the dimerization of the adsorbed molecules of (*R*)-Naproxen (the ratio $2K_{dim}/b_R$ is large), the equilibrium of dimerization progressively shifts towards a monomolecular adsorbed complex when the methanol concentration in the mobile phase increases.

5. Conclusions

The adsorption of the two Naproxen enantiomers on Whelk-O1 CSP follows somewhat different retention mechanisms, as is illustrated by the different shapes of their elution profiles when the methanol concentration of the mobile phase is high. These results are best explained by an adsorption model that assumes: (1) the existence of enantioselective and nonselective adsorption sites; (2) the formation of a monomolecular adsorption complex for the more retained enantiomer; and (3) that of both monomolecular

and bimolecular adsorption complexes for the less retained enantiomer. The bimolecular adsorption complex is supposed to be due to the interaction of a first adsorbed molecule with a second one from the mobile phase.

The surface of Whelk-O1 CSP is hydrophobic. In contact with methanol–water solutions, the grafted organic phase is separated from the bulk liquid by the adsorbed layer enriched with methanol. The mobile phase composition influences adsorption in several ways. It determines the extent of the dimerization of the less retained enantiomer on the surface. The methanol concentration controls the degree of solvation of the adsorbate in the mobile phase, hence the values of the adsorption coefficients. The buffer system concentration controls the saturation capacity of the selective adsorption sites. Although the methanol/water ratio in the adsorbed layer does not significantly vary within the range of mobile phase compositions investigated, the distribution of the buffer additives between the two phases is likely to be influenced by this ratio. Thus, it affects the local pH of the adsorbed layer that may differ from the mobile phase pH. Due to the complexity of the underlying processes, their exhaustive understanding is still to be achieved. The application of the methods of solution chemistry to address the problem of the interactions of Naproxen molecules in the bulk solution is desirable.

Other questions of importance were left untouched in this study, such as the participation of the Naproxen anions to adsorption, the distribution of the buffer components between the mobile and the stationary phases and its effect on adsorption, and the solvation of Naproxen in the adsorbed layer. These challenges should be addressed in further investigations.

The study of reversed-phase chromatography on Whelk-O1 remains hindered by the degradation of the adsorbent in contact with methanol–water buffer solutions and aqueous acidic solutions, particularly at temperature above ca. 35 °C. Reports of applications of Whelk-O1 columns under similar but not identical conditions suggest that the margins of stability of this stationary phase are not yet well defined. One can assert with certainty that this column does not tolerate well the combined use of a high temperature and of acetic acid solutions, but the factors leading to the degradation of this adsorbent in buffers of moderate pH in aqueous solutions of organic solvents are obscure.

Acknowledgements

This work was supported by grant CHE-06-08659 of the National Science Foundation and by the cooperative agreement between the University of Tennessee and the Oak Ridge National Laboratory. L.A. also thanks the Council on Grants at the President of the Russian Federation for support (grant for young scientist MK-3723.2008.3). The authors highly appreciate the generous gift of a column by Regis Technologies (Morton Grove, IL, USA) and thanks Christopher Welch (Merck Research Laboratories, Rahway, NJ) and Ted Szczerba (Regis Technologies) for fruitful discussions.

Appendix A. Calculation of the dissociation degree of Naproxen

We assume that the pH of the mobile phase is determined by the concentration of the acetic buffer system. This means that the dissociation of Naproxen, owing to its low concentration, does not contribute noticeably in the total proton concentration. We also assume that the ionic strength I of the mobile phase is determined only by the concentration of the sodium acetate buffer and remains constant during the elution of the entire band. Hence, the mobile phase pH ($^{s}_{s}$pH) remains constant over the whole column at any moment of time. Let the concentrations of protons, anions, and neutral species of Naproxen and the respective activity coefficients be c_H, c_{Np}, c_{HNp} and γ_H, γ_{Np}, and γ_{HNp}, respectively. Making the usual assumption that $\gamma_{HNp} = 1$ and taking into account that $\log(c_H\gamma_H) = -^{s}_{s}\mathrm{pH}$ one obtains for the dissociation degree:

$$\frac{\alpha}{1-\alpha} = \frac{c_{Np}}{c_{HNp}} = \frac{K_a}{10^{-^{s}_{s}\mathrm{pH}}\gamma_{Np}} = \frac{1}{\gamma_{Np}} 10^{(^{s}_{s}\mathrm{pH} - ^{s}_{s}\mathrm{p}K_a)} \quad (25)$$

where K_a is the dissociation constant of Naproxen (Table 1).

The activity coefficient γ_{Np} was computed using the Debye–Hückel equation:

$$\log(\gamma_{Np}) = -\frac{Az^2\sqrt{I}}{1 + Ba_0\sqrt{I}} \quad (26)$$

where z is the charge of the ion (± 1), and A and B are coefficients depending on the temperature and the mobile phase composition. Their numerical values are listed in [37]. The ion size parameter a_0 was assigned the value of 6.3 proposed for aromatic acids in water–methanol solvents [56]. Calculations were performed for a temperature of 25 °C.

References

[1] W.H. Pirkle, Ch.J. Welch, J. Liq. Chromatogr. 15 (1992) 1947.
[2] Ch.J. Welch, J. Chromatogr. A 666 (1994) 3.
[3] W.H. Pirkle, Ch.J. Welch, J. Chromatogr. A 683 (1994) 347.
[4] W.H. Pirkle, Ch.J. Welch, Tetrahedron: Asymmetry 5 (1994) 777.
[5] Ch. Wolf, W.H. Pirkle, Tetrahedron 8 (2002) 3597.
[6] M.E. Koscho, P.L. Spence, W.H. Pirkle, Tetrahedron: Asymmetry 16 (2005) 3147.
[7] G.E. Job, A. Shvets, W.H. Pirkle, S. Kuwahara, M. Kosaka, Y. Kasai, H. Taji, K. Fujita, M. Watanabe, N. Harada, J. Chromatogr. A 1055 (2004) 41.
[8] A.D. Rio, J.M. Hayes, M. Stein, P. Piras, C. Roussel, Chirality 16 (2004) S1.
[9] C.F. Zhao, N.M. Cann, Anal. Chem. 80 (2008) 2426.
[10] J. Dungelova, J. Lehotay, J. Cizmarik, D.W. Armstrong, J. Liq. Chromatogr. 26 (2003) 2331.
[11] R.W. Stringham, J.A. Blackwell, Anal. Chem. 68 (1996) 2179.
[12] B. Shen, X. Xu, J. Chen, X. Zhang, B. Xu, Chirality 18 (2006) 757.
[13] B.H. Shao, X.Z. Xu, Q.Z. Wu, J.D. Lu, X.Y. Fu, J. Liq. Chromatogr. 28 (2005) 63.
[14] Ch.J. Welch, Chem. New Zeal. 57 (1993) 9.
[15] S. Sergeyev, F. Diederich, Chirality 18 (2006) 707.
[16] A.M. Blum, K.G. Lynam, E. Nicolas, Chirality 6 (1994) 302.
[17] Ch.J. Welch, T. Szczerba, S. Perrin, J. Chromatogr. A 758 (1997) 93.
[18] W.H. Pirkle, M.E. Koscho, J. Chromatogr. A 761 (1997) 65.
[19] J. Zheng, S.A. Shamsi, J. Chromatogr. A 1005 (2003) 177.
[20] J.H. Kennedy, J. Chromatogr. A 725 (1996) 219.
[21] J. Dungelova, J. Lehotay, J. Krupčik, J. Cižmarik, D.W. Armstrong, J. Sep. Sci. 27 (2004) 983.
[22] J. Dungelova, J. Lehotay, J. Krupčik, J. Cižmarik, T. Welsch, D.W. Armstrong, J. Chrom. Sci. 42 (2004) 135.
[23] F. Gritti, G. Guiochon, J. Chromatogr. A 1099 (2005) 1.
[24] J.W. Gibbs, Collected Works, vol. 1, Longmans, London, 1928.
[25] Y.V. Kazakevich, R. LoBrutto, F. Chan, T. Patel, J. Chromatogr. A 913 (2001) 75.
[26] E.A. Guggenheim, Thermodynamics, North-Holland, Amsterdam, 1967, p. 46.
[27] T. Fornstedt, P. Sajonz, G. Guiochon, Chirality 10 (1998) 375.
[28] L. Ravald, T. Fornstedt, J. Chromatogr. A 908 (2001) 111.
[29] G. Götmar, B.J. Stanley, T. Fornstedt, G. Guiochon, Langmuir 908 (2003) 111.
[30] Y.V. Kazakevich, H.M. McNair, J. Chromatogr. Sci. 31 (1993) 317.
[31] CRC Handbook of Chemistry and Physics, 68th ed., R.C. Weast (Ed.), CRC Press, Boca Raton, FL, 1987.
[32] B. Gonzáles, N. Calvar, E. Gómez, A. Domíngez, J. Chem. Thermodyn. 39 (2007) 1578.
[33] J. Samuelsson, J. Zang, A. Murunga, T. Fornstedt, P. Sajonz, J. Chromatogr. A 1194 (2008) 205.
[34] J.H. Knox, R. Kaliszan, J. Chromatogr. 349 (1985) 211.
[35] F. Gritti, Y. Kazakevich, G. Guiochon, J. Chromatogr. A 1161 (2007) 157.
[36] R. Bates, Determination of pH. Theory and Practice, John Wiley and Sons, New York, 1964.
[37] I. Canals, F.Z. Oumada, M. Roseś, E. Bosch, J. Chromatogr. A 911 (2001) 191.
[38] J.Å. Jönsson, P. Lövkvist, J. Chromatogr. 406 (1987) 1.
[39] S.N. Lanin, M.Yu. Ledenkova, Yu.S. Nikitin, Mendeleev Commun. 10 (2000) 37.
[40] G. Guiochon, A. Felinger, A.M. Katti, S.G. Shirazi, Fundamentals of Preparative and Nonlinear Chromatography, 2nd ed., Academic Press, Boston, MA, 2006.
[41] K. Kaczmarski, M. Mazzoti, G. Storti, M. Morbidelli, Computers Chem. Eng. 21 (1997) 641.
[42] A. Felinger, A. Cavazzini, G. Guiochon, J. Chromatogr. A 986 (2003) 207.
[43] J.C. Nash, Compact Numerical Methods for Computers: Linear Algebra and Function Minimisation, Adam Hilger, Bristol, 1990, p. 215.
[44] W. Pirkle, Ch.J. Welch, S.R. Wilson, Chirality 6 (1994) 615.
[45] D.H. Everett, J. Chem. Soc., Faraday Trans. I 60 (1964) 1803.
[46] F. Gritti, G. Guiochon, Anal. Chem. 77 (2005) 4257.

[47] S. Golshan-Shirazi, G. Guiochon, Anal. Chem. 61 (1989) 2380.
[48] R. Arnell, P. Forssén, T. Fornstedt, Anal. Chem. 79 (2007) 5838.
[49] P. Forssén, R. Arnell, M. Kaspereit, A. Seidel-Morgenstern, T. Fornstedt, J. Chromatogr. A 1212 (2008) 89.
[50] J. Navrocki, J. Chromatogr. A 779 (1997) 29.
[51] F. Gritti, G. Guiochon, J. Chromatogr. A 1216 (2009) 1776.
[52] F. Gritti, G. Guiochon, J. Chromatogr. A 1216 (2009) 63.
[53] A. Seidel-Morgenstern, J. Chromatogr. A 1037 (2004) 255.
[54] G. Perlovich, S. Kurkov, A. Kinchin, A. Bauer-Brand, Eur. J. Pharm. Biopharm. 57 (2004) 411.
[55] C.P. Mora, F. Martinez, J. Chem. Eng. Data 57 (2007) 1933.
[56] A. Avdeef, J.E.A. Comer, S.J. Thomson, Anal. Chem. 65 (1993) 42.
[57] F.Z. Oumada, C. Ràfols, M. Rosés, E. Bosch, J. Pharm. Sci. 91 (2002) 991.